Jitian Song[1,2] / Yongxia Feng[1] / Wei Tian[1,2] / Jianbo Liu[1] / Yening Wang[1] / Xiaofei Xu[1]

Enhancement of Heat Transfer Performance Using Ultrasonic Evaporation

[1] Tianjin Key Laboratory of Integrated Design and On-line Monitoring for Light Industry & Food Machinery and Equipment, College of Mechanical Engineering, Tianjin University of Science and Technology, Tianjin 300222, China, E-mail: songjt@tust.edu.cn

[2] International Science and Technology Cooperation Base of Low-Carbon Green Process Equipment, Tianjin 300222, China, E-mail: songjt@tust.edu.cn

Abstract:
The ultrasonic evaporator is a new type of evaporation equipment which uses ultrasonic technology to assist evaporation of liquid materials. Due to the lack of mechanism of ultrasonic technology to enhance the heat transfer in evaporation process, there are few reports on the use of ultrasonic evaporator in industrial production. The tap water was selected as experimental material and the heat transfer performance of ultrasonic evaporator was studied. It could be obtained from the single factor analysis that the heat transfer coefficient increased first and then decreased with the increase of ultrasonic power density. The increase of heat transfer due to the increase of temperature difference is basically stable at 20 %. When the ultrasonic wave acts on evaporator, the heat transfer coefficient would increase about 17.06 %–29.85 %. According to the orthogonal test and analysis of variance, it can be obtained that the influence of temperature difference on heat transfer coefficient is the largest, the second is feed flow rate, and evaporation time has the least influence.

Keywords: ultrasonic evaporation, heat transfer enhancement, regression model

DOI: 10.1515/ijfe-2018-0337

Received: October 11, 2018; **Revised:** February 23, 2019; **Accepted:** March 18, 2019

1 Introduction

With the increasing demand for energy, human beings are facing the problem of energy crisis [1]. How to improve the efficiency of energy utilization, and reduce energy consumption has become a focus all over the world. Heat transfer processes are widely used in a lot of industrial applications, such as oil, chemical, gas, and food industries [2]. For example, liquid foods are often concentrated to reduce energy consumption during subsequent drying, to otherwise facilitate such drying, to induce crystallization, to reduce the weight and volume of products and thereby reduce packaging, transportation and storage costs. [3] Evaporator is a very important heat transfer unit for process industry, and the design and research of high efficiency and energy saving in evaporation is particularly important [4]. The knowledge of a good understanding of the heat transfer characteristics is of great importance to the operation of evaporator [5]. Among the new emerging techniques that could be developed and optimized in order to improve heat transfer processes, the use of ultrasound seems to be one of these new sustainable technical solutions [2]. Ultrasound is an oscillating sound pressure wave with a frequency higher than the upper limit of the human hearing range which is 20 kHz [6]. Propagation of ultrasonic waves induces some fluid dynamic phenomena such as acoustic cavitation and acoustic streaming which are the most significant ones [7]. The collapse of bubbles caused by cavitation produces intense local heating and high pressures, with very short lifetimes. [8]Based on previous researches, cavitation bubbles cause some physical effects such as microstreaming, microjets, shock waves that all of them create turbulency at micro-scale through the medium [9–13].

Due to the unique properties of ultrasound, the ultrasonic technology can be coupled into the solution evaporation process. At present, the researches on the mechanism of heat and mass transfer enhancement under external field are not mature enough and most of them are in the stage of experimental exploration. The theoretical researches of ultrasound abroad are mainly focused on the instantaneous high temperature and high pressure produced by ultrasonic in cavitation, and the ultrasonic products are seldom developed in combination with the characteristics of ultrasonic wave, which is unfavorable to the combination of acoustic chemistry and other subjects in recent years. [14, 15] Saadah and Kang et al. [16–18] have explored the mechanism of ultrasonic wave, especially in the physical and chemical effects of ultrasonic, which provides a theoretical basis for the

Jitian Song is the corresponding author.
© 2019 Walter de Gruyter GmbH, Berlin/Boston.

Automatically generated rough PDF by *ProofCheck* from River Valley Technologies Ltd.

Brought to you by | Göteborg University - University of Gothenburg
Authenticated
Download Date | 11/24/19 11:44 AM

mechanism optimization of ultrasonic and evaporation process. Bergles and Newell [19] studied the increment of heat transfer to the flowing water in annuli using ultrasonic vibration. The results showed that the maximum enhancement in local heat transfer coefficient was 40 % that was occurred in non-boiling condition with low flow rate and high heat flux. Baffigi and Bartoli [20] reported decrement effect of ultrasonic waves on saturated pool boiling heat transfer. They declared that in saturation condition, the cavitation was not happened and this decreasing effect was due to presence of the great amount of vapor that interferes with ultrasonic propagation in the medium. The influence of 2 MHz ultrasonic wave on enhancement of heat transfer from a heating plate to water flowing on it was studied at different Re number by Sauret et al. [21] The results proved that strong influence of acoustic streaming unlike poor acoustic cavitation effects. More turbulence induced by acoustic streaming was the reason of heat transfer enhancement in presence of ultrasonic waves.

In view of the effects of acoustic cavitation in enhancing convective heat transfer and boiling heat transfer, acoustic cavitation enhancement of heat transfer by evaporation has been widely concerned by some scholars. Aijun Hu [22] used 20 kHz ultrasonic power of 2000 W to pretreat the concentrated sugar solution. The results indicated that the heat transfer coefficient and evaporation intensity of the evaporation system were improved by 42.4 % and 15.2 %, respectively. Maryam and Masoud [23] carried out an investigation on the evaporation rate of a novel proposed ultrasonic falling film flowing on a non-heated plate was performed and compared to that of a plain falling film. For this purpose, five 28 kHz ultrasonic transducers were installed underneath of an inclined steel flat plate to irradiate the ultrasonic waves to the film of sodium chloride solution passing upon it. The results showed the effects of ultrasonication on evaporation rate at different temperatures. Induced physical effects, which are caused by size pulsation and collapse of cavitation bubbles, led to evaporation rate enhancement at lower temperatures. However, at higher temperatures, coarse bubbles attached to the plate surface and by reduction of the ultrasound vibrations resulted to reduce the evaporation rate compared to falling film. The highest effect on evaporation rate enhancement was 353 % which was obtained at 40 °C at the lowest Reynolds number of 250. Wang Xiao et al. [24] combined the ultrasonic atomizer and ultrasonic reaction tank with a frequency of 1.7 MHz, and designed and constructed an ultrasonic assisted seawater evaporation test rig. The experimental results show that compared with the natural evaporation, ultrasound has obvious enhancement effect on evaporation, and the evaporation rate increases with the increase of temperature. According to Jiang Bingchen's [25] molecular measurement experiment, it is found that under the same time and ultrasonic power, the ultrasonic wave with a frequency of 40 kHz is better than the frequency of 28 kHz, and at the same time and frequency, the higher the power of the ultrasonic wave, the better the cracking effect.

According to the characteristics of ultrasonic wave and the forced circulating evaporator, a set of ultrasonic evaporation device was designed and manufactured, and the process flow suitable for the ultrasonic evaporation device was set up. The heat transfer performance and internal mechanism of the pure water in the evaporation and concentration process under the aid of ultrasonic wave are mainly studied. Moreover, the appropriate ultrasonic intensification of the evaporation heat transfer operating parameters is determined. The main research contents are as follows:

1. Considering the characteristics of ultrasonic wave and the evaporation characteristics of the forced circulating evaporator, the position of the ultrasonic transducer in the evaporator is determined, and a new type of ultrasonic assisted evaporation device is designed.

2. The relationship between the heat transfer coefficient of the ultrasonic evaporator and the factors such as the evaporation temperature, the heat transfer temperature difference, the ultrasonic power density, the feed flow rate and so on is studied by the single factor method.

3. The main factors and sensitivities affecting the heat transfer enhancement by ultrasonic wave were discussed by the response surface methodology, and the regression model was calculated by the Minitab program. The best regression model was selected, and the best operation parameters of ultrasonic enhanced evaporation process were obtained, providing basic data for the design of ultrasonic evaporator.

2 Materials and methods

2.1 Experimental set-up

The ultrasonic evaporation device used in this experiment is jointly developed by our research group and Tianjin Wuhuan Brothers Pressure Company. The evaporator is coupled with an ultrasonic generator and transducer on the basis of the traditional central circulation tubular evaporator. The evaporation process flow chart of the ultrasonic evaporation device is shown in Figure 1. The evaporator is the main component of the evaporation

Automatically generated rough PDF by *ProofCheck* from River Valley Technologies Ltd

Brought to you by | Göteborg University - University of Gothenburg
Authenticated
Download Date | 11/24/19 11:44 AM

system. The material of the evaporator is stainless steel with a diameter of 20 mm × 2.5 mm. The inner wall of the tube is strictly polished and the effective heating length is 0.5 m. Evaporator is divided into foam chamber, evaporation chamber and heating chamber from top to bottom. The condenser is a 2-pass straight-tube heat exchanger in which the coolant is tap water. Pure water was selected as the experimental material in the experiment.

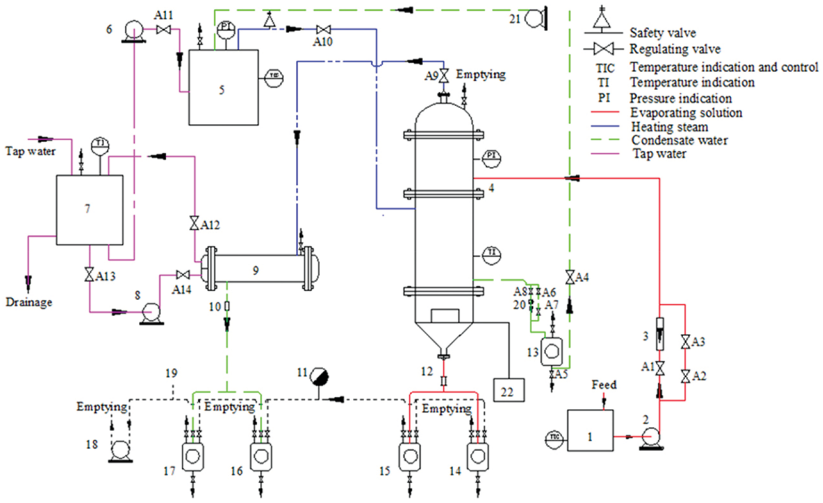

Figure 1: Flow diagram of ultrasonic evaporator.

1-Feed preheating tank 2-Centrifugal pump 3-Rotor flowmeter 4-Ultrasonic evaporator 5-Steam boiler 6-Pipe booster pump 7-Water tank 9-Condenser 10, 12-Sight glass 11-Vacuum meter 13-Condensing tank 1 4, 15-Complete liquid storage tank 16, 17-Condensing tank 18-Vacuum pump 19-Vacuum connected pipeline 20-Drain valve 8, 21-Pipe booster pump

In the experiment, the material (tap water) is heated to the near boiling temperature through the storage tank 1 and then is pumped by the centrifugal pump 2. After the rotor flowmeter 3, it reaches the heating chamber of the lower end of the evaporator 4. The material (tap water) flows from the bottom of the distributor to the end surface of the evaporator after overflowing from the feed pipe, and then flows down the inner wall of the tube. The heating area of the unit volume solution in the heating pipe is larger than the solution in the circulating tube, and the solution vaporization amount is to make the density of the solution in the heating pipe smaller than that in the circulating tube. The density difference causes the solution to fall along the circulating tube and rise along the heating tube to complete the circulation movement. Thus the solution is heated and evaporated repeatedly in the heating chamber. The solution is heated circulated in the evaporation tube and generates secondary steam. The secondary steam condenses through condenser 9 and enters the condensate tank 16 for metering. The concentrated material flows into the storage tank 14, and the metering is carried out to calculate heat transfer coefficient. The water ring vacuum pump 18 ensures the vacuum degree required for the evaporation system and the condensing system. Considering the possibility of producing non-condensable gas in the whole evaporation system, the exhaust port is set up in the jacket of the evaporator and the shell side of the condenser. All experiments were performed in triple.

2.2 Heat transfer coefficient

In engineering practice, it is difficult to obtain the theoretical heat transfer coefficient of evaporation process. In order to obtain the relationship between the heat transfer coefficient of the ultrasonic evaporation process and the operating parameters (feed flow rate, evaporation temperature, heat transfer temperature difference and ultrasonic power density), the average heat transfer coefficient is taken as the measured value by repeated experiments. The calculation equation is as follows:

$$K = \frac{Q}{\mathrm{A}\,\mathrm{d}T} \tag{1}$$

where K is average heat transfer coefficient of evaporation process, W/m^2·°C; Q is the heat transferred by the evaporation wall in a unit time, W; A is the total heat transfer area of this evaporator, m^2; dT is average heat transfer temperature difference, °C.

Automatically generated rough PDF by *ProofCheck* from River Valley Technologies Ltd

Brought to you by | Göteborg University - University of Gothenburg
Authenticated
Download Date | 11/24/19 11:44 AM

In this experiment, the pressure and temperature of heated steam are measured by pressure gauges and thermocouples installed in steam boilers. The temperature of liquid feed is measured by thermocouples installed in preheaters. The flow of feed is measured by rotameter 3, and the evaporation temperature is measured by thermocouples. At the end of each experiment, the volume of liquid in tank 16 and tank 13 was measured separately, and the quantity of secondary steam condensate and heated steam condensate could be obtained. Thereby, the heat transfer Q could be calculated.

2.3 Central composite design method

The central composite design (CCD) method is one of the response surface design methods. It is a test design method developed on the basis of two-level full factor and part of the test design. In order to evaluate the nonlinear relationship between the evaluation index (output variables) and the factors, it is often used to test the nonlinear influence of the factors. Because the CCD has more tests than the orthogonal design and the uniform design, the predictability of the nonlinear fitting model is usually better than the orthogonal design and the uniform design. The CCD method can extend the relationship between various factors and heat transfer coefficient to curved surface. After fitting, the best effect region can be selected from the effect surface by describing the effect surface of curved surface effect on each factor, and the value range of each factor can be predicted, thus ensuring higher experimental accuracy and predictability [26].

3 Results and discussion

3.1 Influence of ultrasonic power density on heat transfer coefficient

Figure 2 shows the effect of ultrasonic power density on heat transfer coefficient of the water evaporation process when the evaporation temperature is taken as 85 °C, the heat transfer temperature difference is 25 °C, and the treatment capacity is 40 L/h. It can be seen from Figure 2 that the heat transfer coefficient gradually increased from 822.4 W/m^2·°C to 1030.4 W/m^2·°C, then gradually decreased to 962.7 W/m^2·°C, with the increase of the ultrasonic power density. This is because the tensile effect of ultrasound on the cavitation core is strengthened at the positive pressure phase of the ultrasonic as the ultrasonic power density increases, and the increase of the radius of the cavitation core is accelerated. In the negative pressure phase of the ultrasonic, the compression of the cavitation nucleus is strengthened and the radius reduction of the cavitation nucleus is also accelerated. This aggravates the movement of the cavitation bubble and the rupture of the cavitation bubble, and increases the pressure difference between the liquid and the vaporization bubble, and thus reduces the nucleation potential barrier of the gas nucleus. The number of bubbles and the frequency of bubble formation are increased. The cavitation phenomenon also promotes the bubble detachment movement and reduces the surface tension of the solution [27]. Accordingly, this would accelerate the disturbance of the fluid in the boundary layer and increase the circulation speed of the fluid in the evaporator, the degree of membrane turbulence and the exchange degree of the internal energy of the liquid. Hence, this cavitation would intensity the heat transfer in the evaporator.

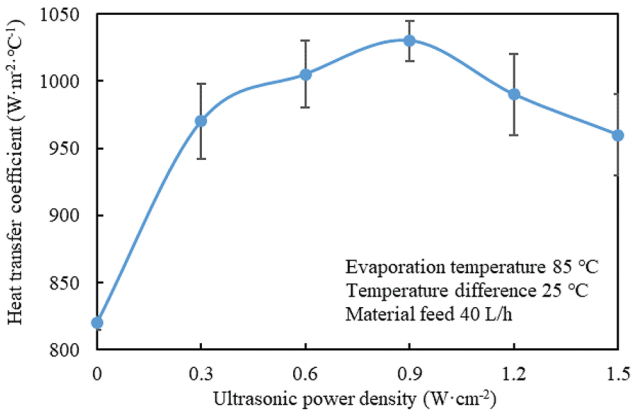

Figure 2: Ultrasonic power density impacts on heat transfer coefficient.

Automatically generated rough PDF by *ProofCheck* from River Valley Technologies Ltd

Brought to you by | Göteborg University - University of Gothenburg
Authenticated
Download Date | 11/24/19 11:44 AM

3.2 Influence of temperature difference on heat transfer coefficient

Figure 3 shows the effect of heat transfer temperature difference on the heat transfer coefficient when the evaporation temperature is 85 °C, the feed flow is 40 L/h, and the ultrasonic power density is 0 and 0.9 W/cm^2 respectively. According to the diagram, the heat transfer coefficient of the ultrasonic evaporator slowly decreases with the increase of heat transfer temperature difference, and then decreases rapidly. This is because with the increase of heat transfer temperature difference, the superheat of bubbles in the evaporating tube increases and the evaporation strength decreases. However, with the further increase of the temperature difference, the liquid film changes from the nucleation boiling to the membrane boiling, the gas film on the evaporating wall thickens. As a result, the thermal resistance of the gas phase increases, the liquid film of the condensing side is thickened and the heat transfer intensity is reduced. It hinders the heat transfer of liquid film and aggravates the reduction of heat transfer coefficient.

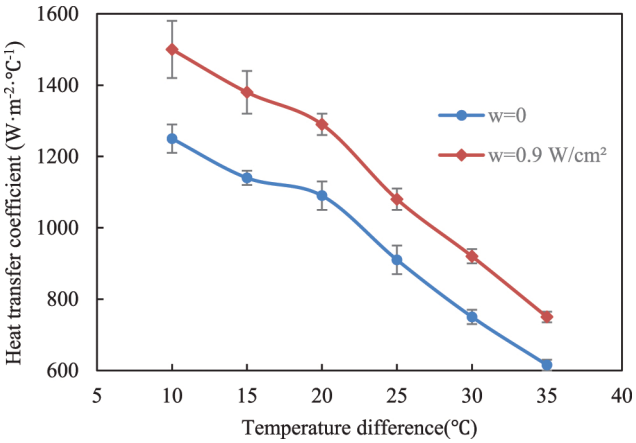

Figure 3: Temperature difference impacts on heat transfer coefficient.

3.3 Regression equations of overall heat transfer coefficient from central composite experiment

The central compound experiment method can extend the relationship between the factors and the heat transfer coefficient to the surface. After fitting the response surface of each factor by describing the effects, the best response area is selected from the response surface, and the range of the value of each factor is predicted, thus the higher experimental accuracy is ensured. Table 1 shows the effect of evaporation temperature, feed flow rate, ultrasonic power density and heat transfer temperature difference on heat transfer coefficient using the CCD method.

Table 1: Central composite design experiments.

S/N	Evaporation temperature T/°C	Feed flow rate L/L·h^{-1}	Power density w/W·cm^{-2}	Temperature difference dT/°C	Heat transfer coefficient K/W·m^{-2}·°C^{-1}	Fitting value
1	70	35	0.3	25	718.5	735.7
2	80	35	0.3	25	856.4	877.6
3	70	45	0.3	25	792.8	779.1
4	80	45	0.3	25	953.8	946.8
5	70	35	0.9	25	817.0	815.5
6	80	35	0.9	25	905.1	902.4
7	70	45	0.9	25	866.2	861.0
8	80	45	0.9	25	963.5	973.7
9	70	35	0.3	35	656.6	651.1
10	80	35	0.3	35	710.9	713.2
11	70	45	0.3	35	670.4	670.2
12	80	45	0.3	35	752.0	758.1
13	70	35	0.9	35	677.3	681.3
14	80	35	0.9	35	669.9	688.4
15	70	45	0.9	35	718.8	702.4
16	80	45	0.9	35	755.4	735.3
17	65	40	6.0	30	727.5	739.1

Automatically generated rough PDF by *ProofCheck* from River Valley Technologies Ltd.

Brought to you by | Göteborg University - University of Gothenburg
Authenticated
Download Date | 11/24/19 11:44 AM

18	85	40	6.0	30	927.4	914.0
19	75	30	6.0	30	727.4	701.6
20	75	50	6.0	30	767.9	791.9
21	75	40	0.0	30	735.5	726.3
22	75	40	1.2	30	775.9	783.4
23	75	40	0.6	20	964.6	956.3
24	75	40	6.0	40	626.9	633.4
25	75	40	0.6	30	824.4	806.0
26	75	40	0.6	30	800.2	806.0
27	75	40	0.6	30	808.3	806.0
28	75	40	0.6	30	816.4	806.0
29	75	40	0.6	30	792.1	806.0
30	75	40	0.6	30	792.1	806.0
31	75	40	0.6	30	808.3	806.0

In order to consider the interaction between various factors and the influence of the second order on the heat transfer coefficient, the response surface regression method is adopted by using the two-degree method. After removing the terms with lower significance level, Table 2 lists the regression coefficient of the model of the heat transfer coefficient. The regression equation is as follows

$K = -1013 - 8.7\ \mathrm{Te} + 43.3\ \mathrm{L} + 1163\ \mathrm{w} + 48.7\ \mathrm{dT} + 0.313\ \mathrm{Te*Te} - 0.485\ \mathrm{L*L} - 143.5\ \mathrm{w*w} - 9.17\ \mathrm{Te*w} - 0.798\ \mathrm{Te*dT} - 8.28\ \mathrm{w*dT}$

Table 2: Regression coefficients of the model.

Term	Coefficient	SE Coefficient	*T*-Value	*P*-Value
Constant	−1013	1146	−0.88	0.387
Te	−8.7	26.3	−0.33	0.743
L	43.3	13.5	3.20	0.004
W	1163	317	3.67	0.002
dT	48.7	17.2	2.83	0.010
Te*Te	0.313	0.169	1.85	0.079
L*L	−0.485	0.169	−2.87	0.009
W*W	−143.5	61.7	−2.33	0.031
Te*W	−9.17	3.79	−2.42	0.025
Te*dT	−0.798	0.227	−3.51	0.002
W*dT	−8.28	3.79	−2.19	0.041
S = 22.7158 PRESS = 26,276.3 R^2 = 95.86 %				
R^2 (pred) = 89.45 % R^2 (adj) = 93.79 %				

Table 2 and Table 3 show that regression coefficients of the model and variance analysis of the heat transfer coefficient. As can be seen from Table 2, the model accuracy coefficient R^2 is 95.86 % and adjusted R^2 is 93.79 %, which are close to 1. The corresponding predicted R^2 is 89.45 %, large and close to 1, which indicates the prediction is credible based on the regression equation. Table 3 shows the *P*-value for the regression model is 0.000, that it should reject the null hypothesis, and this model is effective in general. The *P*-value corresponding to the lack of fit term of this model is 0.85, significantly greater than the significance level of 0.05. It is considered that there is no lack of fit term in this model.

Table 3: Variance analysis of the heat transfer coefficient.

Source	Freedom	Seq SS	Adj SS	Adj MS	F-Value	P-Value
Regression	10	238,835	238,835	23,883.5	46.29	0.000
Te	1	45,868	57	56.8	0.11	0.743
L	1	12,249	5287	5287.1	10.25	0.004
W	1	2916	6955	6955.1	13.48	0.002
dT	1	156,397	4126	4126.4	8.00	0.010
Te*Te	1	2108	1772	1772.4	3.43	0.079
L*L	1	4636	4262	4262.0	8.26	0.009
W*W	1	2792	2792	2792.4	5.41	0.031
Te*W	1	3031	3031	3030.5	5.87	0.025
Te*dT	1	6368	6368	6368.0	12.34	0.002
W*dT	1	2470	2470	2470.1	4.79	0.041
Error	20	10,320	10,320	516.0		

Automatically generated rough PDF by *ProofCheck* from River Valley Technologies Ltd

Brought to you by | Göteborg University - University of Gothenburg
Authenticated
Download Date | 11/24/19 11:44 AM

Lack-of-fit	13	5097	5097	392.1	0.53	0.850
Pure error	7	5223	5223	746.1		
Total	30	249,155				

Notes: pred = prediction adj=adjustment.

Figure 4 illustrates residual diagram of the model and the measured value. From the normal test plots of the residuals of heat transfer coefficients from histogram and normal probability map, we can see that the trend of residual plots is normal distribution. It is evident from the scatter plot that the random fluctuations of the experimental points on the horizontal axis are random, and there is no equal variance, and the trend of bending can be clearly seen from the scatter plot. To sum up, it can be concluded from the residual condition that there is no lack of fit term and bending in the model, which is very consistent with the data, and the difference between the measured value and the predicted value is small.

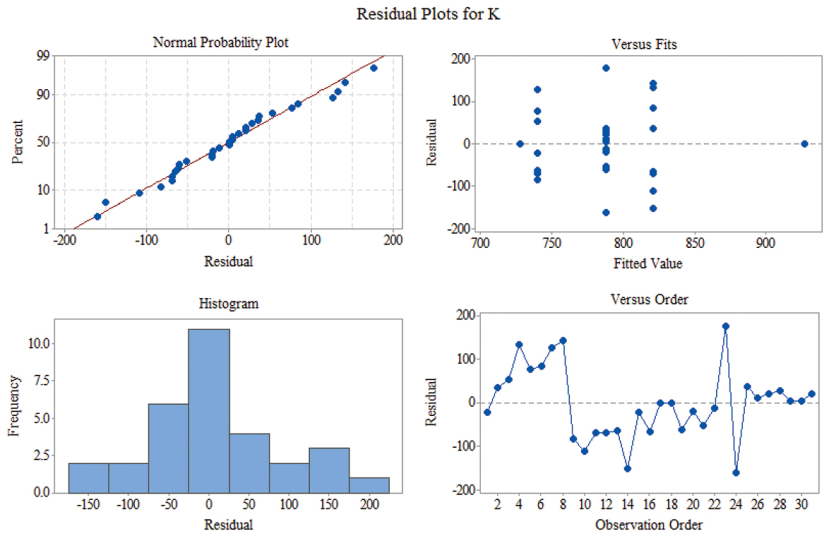

Figure 4: Residual diagram of overall heat transfer coefficient in regression.

3.4 Analysis of overall heat transfer coefficients based on contour plots

Figure 5 shows the contour map of the heat transfer coefficient as a function of evaporation temperature and handling capacity. The ultrasonic power density is set as a constant 0.6 W/cm^2 and the heat transfer temperature difference is taken as 30 °C. It can be seen from the diagram that the heat transfer coefficient increases with the increase of evaporation temperature when the handling capacity is fixed. This is because with the increase of the evaporation temperature, the flow resistance of the liquid decreases, the turbulent degree increases. As a result, the average thickness of the liquid film decreases, the thermal resistance decreases, and the corresponding heat transfer coefficient increases. When the evaporation temperature is constant, the heat transfer coefficient increases first and then decreases with the increase of handling capacity. This is because with the increase of the feed volume, the prolongation of the evaporation section, the increase of the evaporation area, and the acceleration of the liquid film renewal, which all enhance heat transfer in the evaporator. However, as the feed volume continues to increase, the amount of heat used by the evaporator to preheat the material increases, and the heat flux decreases, which makes the heat transfer coefficient slow down.

Automatically generated rough PDF by *ProofCheck* from River Valley Technologies Ltd

Brought to you by | Göteborg University - University of Gothenburg
Authenticated
Download Date | 11/24/19 11:44 AM

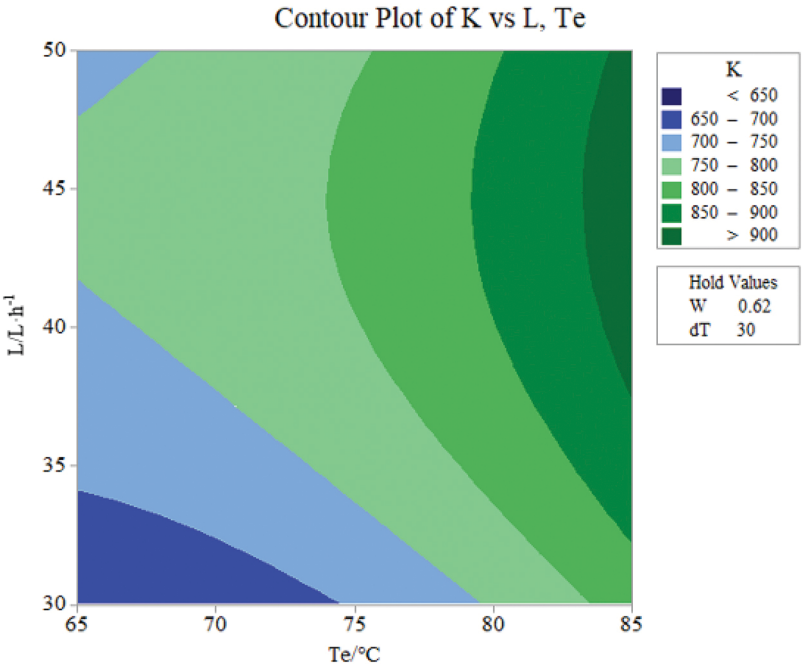

Figure 5: The contour plots of the heat transfer coefficient with handling capacity and evaporation temperature.

Figure 6 shows the contour map of heat transfer coefficient as a function of heat transfer temperature difference and ultrasonic power density. It can be seen from the diagram that the handling capacity is 40 L/h, and the evaporation temperature is 75 °C as the holding values. With the increase of ultrasonic power density, the heat transfer coefficient first increases and then decreases. This is mainly due to the enhancement of the cavitation and atomization in the evaporator and the enhancement of heat transfer with the increase of ultrasonic power density. With the increase of ultrasonic power density to the critical value, the cavitation atomization phenomenon is weakened, the degree of heat transfer enhancement is reduced, and the heat transfer coefficient increases with the increase of evaporation temperature.

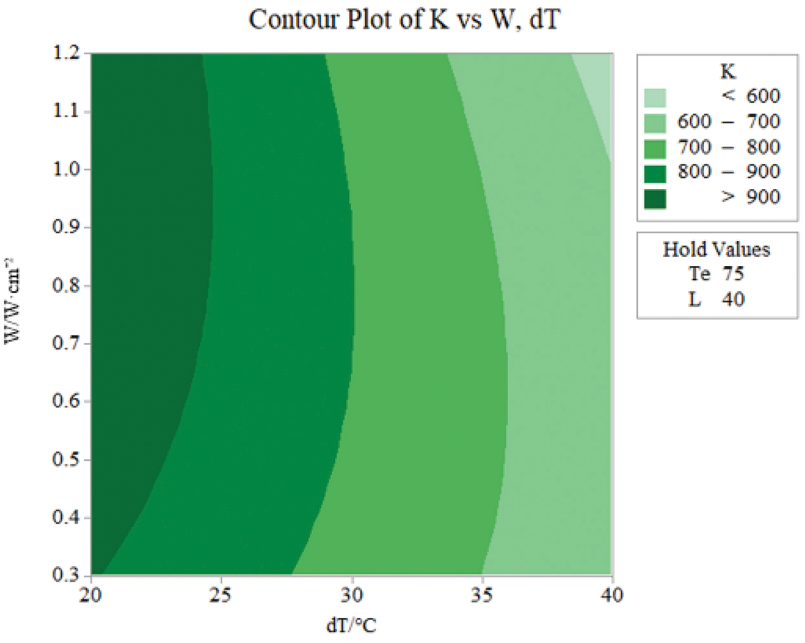

Figure 6: The contour plots of the heat transfer coefficient with heat transfer temperature difference and ultrasonic power density.

Figure 7 shows the contour map of heat transfer coefficient as a function of heat transfer temperature difference and handling capacity. As shown in Figure 7, the heat transfer coefficient decreases with the increase of heat transfer temperature difference. With the increase of heat transfer temperature, the overheat of gas phase increases and the vaporized surface forms gas film, resulting in the increase of the thermal resistance of the gas phase and the thickening of the liquid film on the condensing side, which hinders the heat transfer. The

Automatically generated rough PDF by *ProofCheck* from River Valley Technologies Ltd

Brought to you by | Göteborg University - University of Gothenburg
Authenticated
Download Date | 11/24/19 11:44 AM

heat transfer coefficient increases first and then decreases with the increase of ultrasonic power density, and the change is more obvious when the heat transfer temperature difference is low. This is because with the increase of heat transfer temperature, the number of gasifying bubbles in the heat transfer tube and circulating tube increases sharply, and the fluid rapidly turns into annular flow. The heat transfer is maintained completely by the heat conduction of the liquid film and the natural evaporation of the surface. The temperature of the liquid film on the wall of the heat transfer is gradually reduced, which causes the evaporation solution not to reach the bubble condition, and the gasification bubble is no longer produced. At this time, the cavitation caused by ultrasonic is also gradually weakened, the number of bubbles and the rate of volatilization are further reduced, which leads to the increase of heat transfer temperature difference, and the influence of ultrasonic power density to heat transfer gradually decreases.

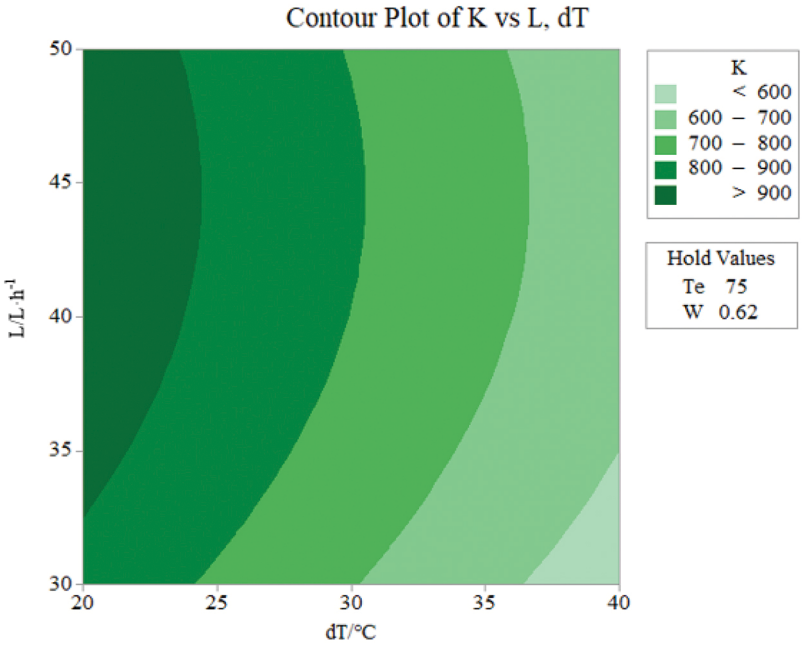

Figure 7: The contour plots of the heat transfer coefficient with handling capacity and heat transfer temperature difference.

Figure 8 shows the contour map of heat transfer coefficient as a function of evaporation temperature and heat transfer temperature difference. It can be seen from the diagram that when the heat transfer temperature difference is low, the heat transfer coefficient increases with the increase of evaporation temperature. This is because the reduction of heat transfer temperature causes the heat flux to decrease. The fluid in the evaporating tube rapidly changes from the membrane boiling to the gaseous boiling. The bubbles are accelerated away from the heating surface, and the film gradually decreases to the disappearance, and the heat transfer performance is gradually increased. With the increase of evaporation temperature, the vaporization strength increases and the disturbing convection increases, the flow resistance of the liquid film decreases. Hence, the eddy diffusion and the heat transfer are strengthened, and the heat transfer coefficient would decrease with the increase of the heat transfer temperature difference.

Automatically generated rough PDF by *ProofCheck* from River Valley Technologies Ltd.

Brought to you by | Göteborg University - University of Gothenburg
Authenticated
Download Date | 11/24/19 11:44 AM

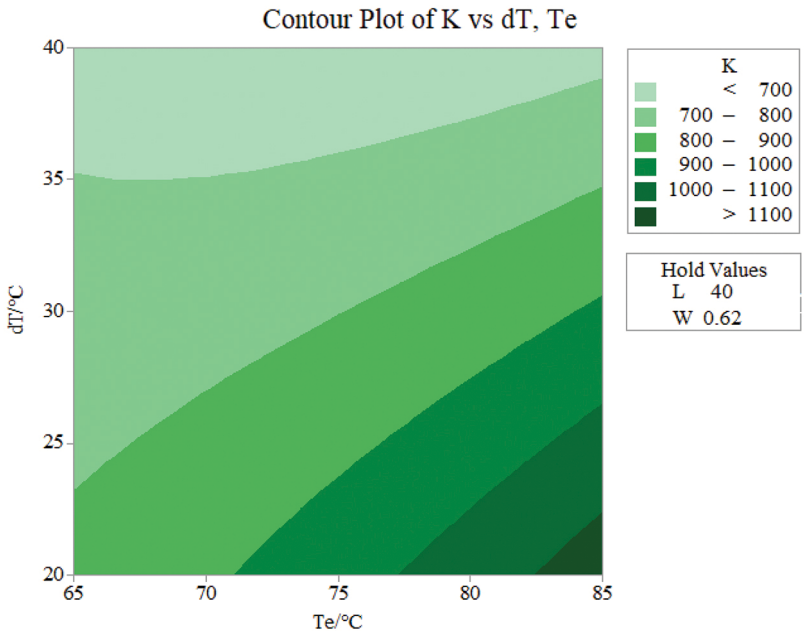

Figure 8: The contour plots of the heat transfer coefficient with evaporation temperature and heat transfer temperature difference.

Figure 9 shows the contour map of heat transfer coefficient as a function of ultrasonic power density and handling capacity. It can be seen from the diagram that the heat transfer coefficient increases first and then decreases with the increase of handling capacity. With the increase of feed flow, the irrigation rate of the evaporation surface increases, the velocity of vaporization in the tube increases and the macro turbulence increases in the evaporation chamber, which all promote the heat transfer effect and increase the heat transfer coefficient. However, with the further increase of feed volume, the average thickness of the liquid film increases and the heat transfer resistance increases. This will reduce the heat transfer enhancement and reduce the heat transfer coefficient. The heat transfer coefficient increases first and then decreases with the increase of ultrasonic power density. This is because with the increase of ultrasonic power density, the cavitation in the evaporation chamber is strengthened, and the degree of micro convection and macro turbulence is enhanced, thus enhancing heat transfer. However, when the ultrasonic power density reaches a critical value, the cavitation phenomenon is suppressed, resulting in a decrease in the amount of foaming in the evaporation tube and a decrease in the gas liquid separation rate, thereby inhibiting heat transfer.

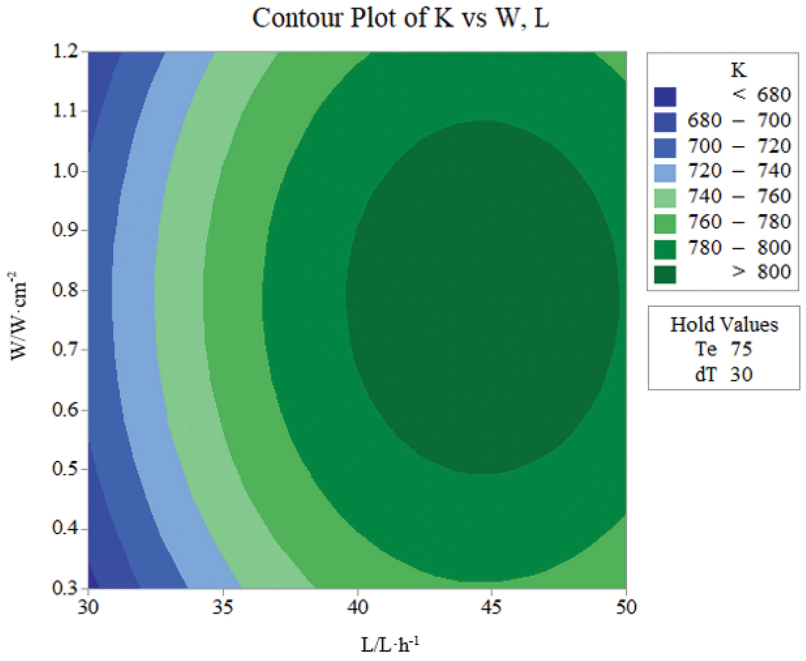

Figure 9: The contour plots of the heat transfer coefficient with handling capacity and ultrasonic power density.

Automatically generated rough PDF by *ProofCheck* from River Valley Technologies Ltd

Brought to you by | Göteborg University - University of Gothenburg
Authenticated
Download Date | 11/24/19 11:44 AM

4 Conclusion

1. The influence of the main parameters on heat transfer in the ultrasonic evaporator is analyzed. The heat transfer coefficient increases first and then decreases with the increase of ultrasonic power density. With the increase of evaporation temperature, the heat transfer coefficient first increases and then tends to be stable. The increase of heat transfer due to the increase of temperature difference is basically stable at 20 %. With the increase of feed flow rate, it slowly increases to 22.55 %. When the ultrasonic wave acts on evaporator, the heat transfer coefficient would increase about 17.06 %–29.85 %.
2. The following conclusion is obtained by orthogonal test and analysis of variance. All the factors are sensitive to the total heat transfer coefficient of the evaporator. The influences from large to small degrees on heat transfer performance in this evaporator are heat transfer temperature difference, evaporation temperature, feed flow rate, and evaporation time.
3. By using the CCD in the response surface analysis, the heat transfer coefficient of the ultrasonic evaporation device is experimentally designed. It is concluded that the evaporation temperature and ultrasonic power density, the interaction between the evaporation temperature and the heat transfer temperature difference also have significant influences on the change of the total heat transfer coefficient. The R^2 (coefficient of determination) of this model is 95.86 %, the adjusted R^2 is 93.79 %, and the predicted R^2 is 89.45 %, which indicates that the regression model is sufficient to represent the relationship among input parameters and heat transfer performance for this ultrasonic evaporator.

Funding

This work was supported by the Hebei Provincial and University Science & Technology Cooperation and Development [grant number 130127] and the Key Project of Philosophy and Social Sciences Research, Ministry of Education (China) "Research on Green Design in Sustainable Development" [grant number 16JZDH014], [grant number 16JZD014].

Symbol list

K Heat transfer coefficient, W/m^2·°C;
Q The heat transferred in a unit time, W;
A The total heat transfer area of evaporator, m^2;
dT Heat transfer temperature difference, °C;
Te Evaporation temperature, °C;
L Feed flow rate, L/h;
w Power density, W/cm^2;

References

[1] Minaei S, Motevali A, Ghobadian B, Banakar A, Samadi SH. An investigation of energy consumption, solar fraction and hybrid photovoltaic-thermal solar dryer parameters in drying of chamomile flower. *Int J Food Eng*. 2014;10:697–711.
[2] Gondrexon N, Cheze L, Jin Y, Legay M, Tissot Q, Hengl N. Intensification of heat and mass transfer by ultrasound: application to heat exchangers and membrane separation processes. *Ultrason Sonochem*. 2015;25:40–50.
[3] Gandhidasan P, Mohammed RC. Concentration of liquid foods using desiccants: an experimental study. *Int J Food Eng*. 1993;17:203–215.
[4] Li JF, Hao JH, Lv JF, Ji HM, Yang D, Huang HT. Status of circulating fluidized bed boiler operation in China. *Boiler Technol*. 2010;41:33–37.(In Chinese).
[5] Song JT, Chi J. Heat transfer enhancement of a three phase circulating fluidized bed fruit juice evaporator using inert particles. Int J Food Eng. 2011;7:192–212.
[6] Gavahian M, Farhoosh R, Javidnia K, Shahidi F, Golmakani MT, Farahnaky A. Effects of electrolyte concentration and ultrasound pretreatment on ohmic-assisted hydro distillation of essential oils from mentha piperita L. *Int J Food Eng*. 2017;13(10):20170010.
[7] Dehbani M, Rahimi M, Abolhasani M, Maghsoodi A, Afshar PG, Dodmantipi AR. CFD modeling of convection heat transfer using 1.7 MHz and 24 kHz ultrasonic waves: a comparative study. *Heat Mass Transfer*. 2014;50:1319–1333.

Automatically generated rough PDF by *ProofCheck* from River Valley Technologies Ltd.

Brought to you by | Göteborg University - University of Gothenburg
Authenticated
Download Date | 11/24/19 11:44 AM

[8] Suslick KS. Sonochemistry. *Science*. 1990;247:1439–1445.
[9] Wu TY, Guo N, Teh CY, Hay JX. Theory and fundamentals of ultrasound, advances. Springer Neth. 2013;52:5–12.
[10] Kuppa R, Moholkar VS. Physical features of ultrasound-enhanced heterogeneous permanganate oxidation. *Ultrason Sonochem*. 2010;17:123–131.
[11] Collis J, Manasseh R, Liovic P, Tho P, Zhu Y. Cavitation microstreaming and stress fields created by microbubbles. *Ultrasonics*. 2010;50:273–279.
[12] Guo G, Ma Y, Guo Y, Zhang C, Guo X, Tu J. Enhanced porosity and permeability of three-dimensional alginate scaffolds via acoustic microstreaming induced by low-intensity pulsed ultrasound. *Ultrason Sonochem*. 2017;37:279–285.
[13] Adewuyi YG. Sonochemistry: environmental science and engineering applications. *Ind Eng Chem Res*. 2001;40:4681–4715.
[14] Niemczewski B. Cavitation intensity of water under practical ultrasonic cleaning conditions. *Ultrason Sonochem*. 2014;3:354–359.
[15] Campos-Pozuelo C, Vanhille C. Electrical detection of the ultrasonic cavitation onset. *Ultrason Sonochem*. 2012;6:1266–1270.
[16] Yusof SM, Babgi B, Alghamdi Y, Aksu M, Madhavan J, Ashokkumar M. Physical and chemical effects of acoustic cavitation in selected ultrasonic cleaning applications. *Ultrason Sonochem*. 2015;13:1–8.
[17] Kang MG. Pool boiling heat transfer on tandem tubes in vertical alignment. *Int J Heat Mass Transf*. 2015;15:138–144.
[18] Li DG. Effect of ultrasonic cavitation on the diffusivity of a point defect in the passive film on formed Nb in 0.5 M HCL solution. Ultrason Sonochem. 2015;18:296–306.
[19] Bergles AE, Newell PH. The influence of ultrasonic vibrations on heat transfer water flowing in annuli. *Int J Heat Mass Transf*. 1965;8:1273–1280.
[20] Baffigi F, Bartoli C. Influence of the ultrasounds on the heat transfer in single phase free convection and in saturated pool boiling. Exp Therm Fluid Sc. 2012;36:12–21.
[21] Bulliard-Sauret O, Ferrouillat S, Vignal L, Memponteil A, Gondrexon N. Heat transfer enhancement using 2 MHz ultrasound. *Ultrason Sonochem*. 2017;39:262–271.
[22] Hu A, Zheng J, Qiu TQ. Industrial experiments for the application of ultrasound on scale control in the Chinese sugar industry. Ultrason Sonochem. 2006;13:229–333.
[23] Dehbani M, Rahimi M. Introducing ultrasonic falling film evaporator for moderate temperature evaporation enhancement. *Ultrason Sonochem*. 2018;42:689–696.
[24] Wang X. *Study on the ultrasound assisted solar energy seawater desalination system*. Qingdao: Qingdao Technological University, , 2010. In Chinese.
[25] Jiang BC, Zhao SS. Physical property study on treatment of engine-oil polluted wastewater by ultrasound. *Environ Sci Technol*. 2014;112–116.(In Chinese).
[26] Zhang WL, Wang YJ, Gao XM, Gao X, Peng SJ, Zheng Y. Optimization of Jiawei Qing'e oral fast disintegrating tablets based on response surface-central composite design. *Chin Herbal Medicines*. 2013;5:138–144.
[27] Zhang ZY, Wang QD, Zhang HS. Numerical investigation of surface tension effects on 2-D cavities near a solid wall. *Theor Appl Mech*. 2005;37:100–104.In Chinese.

Automatically generated rough PDF by *ProofCheck* from River Valley Technologies Ltd

Brought to you by | Göteborg University - University of Gothenburg
Authenticated
Download Date | 11/24/19 11:44 AM